Computers in Biology and Medicine 140 (2022) 105088

Contents lists available at ScienceDirect

Computers in Biology and Medicine

journal homepage: www.elsevier.com/locate/compbiomed

S2FLNet: Hepatic steatosis detection network with body shape

Qiyue Wang [a,*], Wu Xue [b], Xiaoke Zhang [b], Fang Jin [b], James Hahn [a]

[a] Department of Computer Science, The George Washington University, USA
[b] Department of Statistics, The George Washington University, USA

ARTICLE INFO

Keywords:
Dilated residual network
Center loss
Hepatic steatosis

ABSTRACT

Fat accumulation in the liver cells can increase the risk of cardiac complications and cardiovascular disease mortality. Therefore, a way to quickly and accurately detect hepatic steatosis is critically important. However, current methods, e.g., liver biopsy, magnetic resonance imaging, and computerized tomography scan, are subject to high cost and/or medical complications. In this paper, we propose a deep neural network to estimate the degree of hepatic steatosis (low, mid, high) using only body shapes. The proposed network adopts dilated residual network blocks to extract refined features of input body shape maps by expanding the receptive field. Furthermore, to classify the degree of steatosis more accurately, we create a hybrid of the center loss and cross entropy loss to compact intra-class variations and separate inter-class differences. We performed extensive tests on the public medical dataset with various network parameters. Our experimental results show that the proposed network achieves a total accuracy of over 82% and offers an accurate and accessible assessment for hepatic steatosis.

1. Introduction

Fatty liver, also known as hepatic steatosis, occurs when excessive fat accumulates within the liver cells [1]. Hepatic steatosis has been a prominent feature of some of the most common health problems such as Non-Alcoholic Fatty Liver Disease (NAFLD) and Alcoholic Fatty Liver Disease (AFLD) [2]. NAFLD is emerging as one of the most common causes of chronic liver disease, metabolic syndrome, type 2 diabetes and cardiovascular disease [3,4]. Existing literature indicates that with the pandemic spread of obesity, NAFLD affects more than 25% of the population in the developed countries [5–7]. Hepatic steatosis is often reversible in the early stages by appropriate treatments. Therefore, it is of vital importance to detect the presence of steatosis and to assess its severity in order to recognize fat-related functional abnormalities in the liver [8].

Currently, liver biopsy is considered the gold reference standard for diagnosis and grading of hepatic steatosis [9]. Liver biopsy is the procedure in which a small piece of liver tissue is removed and a histological analysis is conducted. However, it is an invasive method and there exists many associated complications (e.g., abdominal pain, internal bleeding, puncture damage to nearby tissue or organs and potential infection). These drawbacks limit liver biopsy being utilized particularly for repeated measurements over time.

Imaging techniques such as computed tomography (CT) and magnetic resonance imaging (MRI) are non-invasive techniques in clinical practice and have important roles in the diagnosis of hepatic steatosis [10,11]. CT scanning is a widely available tool, which provides an assessment of hepatic steatosis using Hounsfield Units (HU) associated with voxels [10]. MRI assesses hepatic steatosis based on its ability to estimate the relative magnitude of the signals arising from fat and water in each voxel [12]. However, MRI and CT scans are expensive and the ionizing radiation exposure associated with CT may be harmful to heath. In addition to CT and MRI scans, there are other clinical approaches to conduct initial/preliminary detection of hepatic steatosis. Patients with hepatic steatosis are more likely to have insulin resistance. In many cases, fatty liver disease is diagnosed after blood tests show elevated liver enzymes alanine aminotransferase and aspartate aminotransferase [13]. Although serum markers provide approaches to detect overall hepatic steatosis, they have poor sensitivity and specificity and correlate poorly with the level of steatosis [14]. The other popular technique is the abdominal ultrasound scan, which uses high-frequency sound waves to capture images to evaluate the size and shape of the liver, as well as blood flow through the liver. In ultrasound images, steatotic livers look brighter than normal livers whereas livers with fat and advance fibrosis look lumpy and shrunken [11,15]. Ultrasound scans have the advantage of safety, wide availability and little associated patient discomfort. In

* Corresponding author.
E-mail address: wangqiyue@gwu.edu (Q. Wang).

https://doi.org/10.1016/j.compbiomed.2021.105088
Received 30 September 2021; Received in revised form 25 November 2021; Accepted 26 November 2021
Available online 30 November 2021

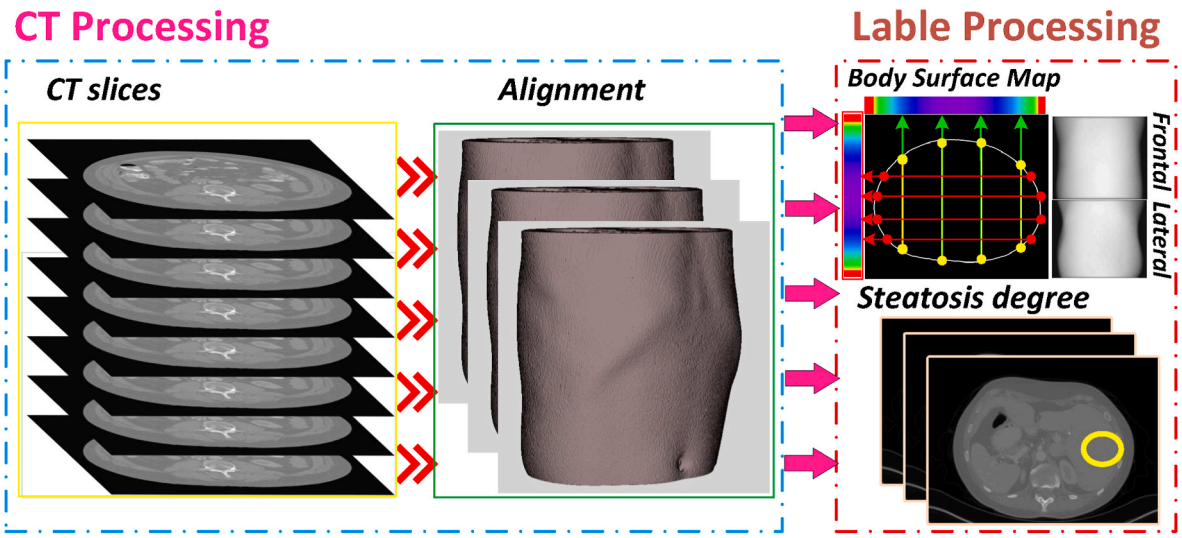

Fig. 1. The extraction pipeline of 2D body shape maps and the degree of hepatic steatosis with CT scans. The original CT scans are calibrated and aligned to a canonical standard in the pipeline. The shape contours extracted from each slice are then combined together to produce the frontal and lateral body shape maps. The degree of hepatic steatosis to be used as the ground truth is estimated by averaging HU values of different liver regions.

addition, the cost of abdominal ultrasound is relatively low compared to CT and MRI. Nonetheless, ultrasound has a relatively poor performance on qualitative classifications of steatosis degrees. There is a very simple physical exam to check for fatty liver by palpating or pressing on patients' abdomen. However, this provides a very rough assessment and is usually used along with other methods [3]. Therefore, there is an increasing interest in developing reliable, inexpensive and non-invasive methods to detect and monitor the progression of hepatic steatosis.

With the explosive growth of optical scan technologies (e.g., using time-of-flight, vision, or structured light) and their availability on commodity devices including smart phones [16–18], body shape has the potential to become an important predictor of a variety of health outcomes. Shape-based anthropomorphic measurements (e.g., body shape index, body roundness index, waist-to-hip ratio and waist-to-height ratio) are associated with the degree of adiposity [19]. However, the relationship between body shape and hepatic steatosis has not been studied. Consequently, we propose a Shape to assess Fatty Liver Network (S2FLNet) to provide a convenient and economical methodology to classify hepatic steatosis.

This paper has three main contributions.

- We propose a body shape based dilated residual network to detect hepatic steatosis. To the best of our knowledge, this is the first work to explore the relationship between the characteristics of body shapes and hepatic steatosis.
- We introduce a center loss along with traditional cross entropy loss to enhance the classification performance by compacting the intra-class variations and separating the inter-class differences.
- We offer a convenient and affordable approach to steatosis assessment which can be made widely accessible.

The remainder of our paper proceeds as follows. The body shape related techniques to predict health outcome are summarized in Related Works. The details of the dataset are introduced in Dataset and Body Shape Representation. The neural network architecture and model processing is presented in Methodology. We demonstrate our implementation details, including hyper-parameters, algorithm validation and prediction accuracy evaluation in Experiment. The paper ends with Conclusion.

2. Related work

Studies show that excess fat in the abdominal area is usually associated with metabolic syndrome and can increase the likelihood of having more advanced forms of liver fat [20,21]. Body Mass Index (BMI) is the most common metric for indicating obesity levels [16,17]. Based on this principle, clinicians use BMI related factors to assess liver fat [13,20]. Although BMI is very easy to calculate, the evaluation accuracy of using BMI is very poor since there is much clinical evidence that indicates a part of non-obese patients are also at risk of fatty liver complications [21]. That is because Visceral Adipose Tissue (VAT) and not all abdominal fat is directly associated with hepatic steatosis [3]. In addition, the relative amount of VAT is small and has little contribution to the overall obesity level. It has been shown that waist circumference is highly correlated with VAT [17,22]. Given the strong associations between liver fat/waist circumference and VAT, early studies have found that waist circumference can be used to assess liver fat [21,23]. According to previous studies [16,24], waist circumference is only one of the shape descriptors and is not sufficient to represent body shape, thus the accuracy is not very high.

Accessibility of 3D human body scanning technologies provide researchers with ways to extract numerous accurate shape related measurements from 3D geometry. In order to investigate correlations between the body shape and various healthy biomarkers [17,25], Xie et al. [26] studied body silhouettes and analyzed the correlation between the variation of shapes and the body leanness indicators; Lu et al. [16] proposed a body fat percentage estimation model by exploring 3D body shape features without anatomical presuppositions. Previous research has shown that VAT is an important intermediary between body shape and liver biomarkers [3,19]. There have been many approaches to predict body fat and VAT volume from the characteristics of body shape [16,17,24,27]. Ng et al. [25] extracted the shape representation from the 3D body surface with principal component analysis (PCA) and provided clinically relevant information to body composition estimates (regional fat/lean masses/VAT). However, these methods adopted simple statistical machine learning models (i.e., Gaussian Process Regression (GPR), Support Vector Machine(SVM), Logistic Regression(LR) etc.) with the discretized shape descriptors. Thus, they are not able to extract deeper shape features resulting in poor predictability. Wang et al. [26] used dilated residual neural network to extract deep and refined features from 2D body shape maps that works well in predicting the 2D pixel level body composition maps. In this work, we

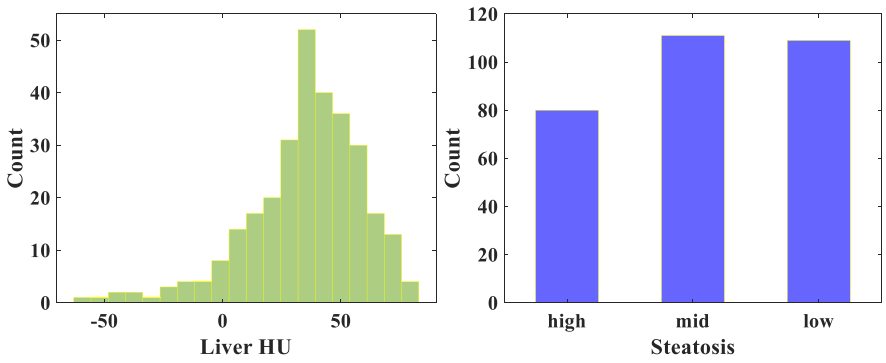

Fig. 2. The histograms of the CT based steatosis assessment. (Left) The distribution of the liver HU values of our dataset. (Right) The distribution of the degree of steatosis based on HU values.

further explore shape descriptors derived from 3D geometries and propose to use deep learning model to map the body shapes to hepatic steatosis.

3. Dataset and body shape representation

The goal of this study is to train a prediction model to classify the steatosis degrees with only body shape and to provide an accurate method to assess hepatic steatosis with body scans. However, optical body scans with the associated degree of hepatic steatosis are not available at this time. CT scan is an accurate method to calculate the degree of hepatic steatosis. The spatial reconstruction precision of CT is very high (0.5 mm–2 mm) compared to commercial optical body scanners (∼ 2 mm). Therefore, we use CT to generate the iso-surface representing the shape of the body as well as the degree of hepatic steatosis for the training set in this study. The main contribution of our work is to provide a validated methodology to map body shapes to hepatic steatosis. The methodology can be used to map body shapes from a variety of sources including optical scanners.

In this section, we give a brief introduction to the medical dataset (Dataset). We also describe the pipeline to extract the input 2D body shape maps (Body Shape Maps) that represent the 3D body shapes and the output degrees of steatosis (Steatosis Degrees).

3.1. Dataset

Liver fat quantification tool for CT has been used for establishing the prevalence of steatosis in a large screening cohort [1,2]. In this study, we use the CT scans from three sources: Cancer Imaging Archive (TCIA) [4,28], Liver Tumor Segmentation Challenge (LiTS) [29] and Combined Healthy Abdominal Organ Segmentation (CHAOS) [30]. Because the raw CT scan data is obtained from different sources and their scan protocols are not the same, it is necessary to calibrate the dataset before extracting the body shape and determining the degree of hepatic steatosis. We manually align all the CT scans and re-sample to ensure CT scan slice thickness and image resolution consistency. All the subject CT data are manually processed via the specialized medical segmentation tool ITK-SNAP [31]. To ensure the reliability of ground truth, we reviewed each subject data at least twice. The dataset (Fig. 1) contains a total of 300 CT scans. Compared with related clinical studies in body fat and metabolism assessment [16,27,32], our sample size is relatively large.

3.2. Body shape maps

CT uses rotating X-ray sources to create cross-sectional images of the body that may also be combined to produce a 3D image of a particular area of the body [29]. The reconstructed 3D body shapes that use CT iso-surfaces are shown in Fig. 1 (left). The 3D body shape is not suitable for being directly fed into our prediction models, thus we transform the original 3D body shape into useable two 2D depth maps without loss of information [17,26]. The protocol is as follows: we first extract the body contour of each CT slice and then decompose their depth values into frontal and lateral directions. Following this, we combine all the resultant slices to obtain the 2D body shape maps in Fig. 1 (top right). In this study, the image size of the 2D body shape maps is 512 × 512.

Table 1
The categorization of steatosis degree with HU values.

Degree	Count	HU range	HU mean	HU std
Low	109	[45.0, 81.4]	57.6	9.0
Mid	111	[25.0, 45.0]	35.4	5.4
High	80	[-61.5, 25.0]	4.3	19.6
Total	**300**	**[-61.5, 81.4]**	**35.2**	**24.1**

3.3. Steatosis degrees

The absolute measured attenuation values at each voxel, i.e., HU, can be used to evaluate steatosis since CT images show decreased attenuation values in the liver parenchyma with fat accumulation [1,2,8]. However, the HU values for liver fat is prone to sampling bias because of the relatively small size of the liver in the image. To avoid sampling errors/bias and to estimate hepatic steatosis more accurately, we collect at least eight liver regions in each slice as shown in Fig. 1 (bottom right) and then average their HU values. We apply the protocol on all the 300 subjects of our dataset. Their HU value distribution is shown in Fig. 2 (left). The severity or the degree of liver fat has a negative linear correlation with its HU value [8]. The degrees of the steatosis can be defined by dividing the subjects into three groups (low, mid, high) based on the HU distribution. The steatosis degrees are not uniformly distributed. In order to obtain well balanced datasets, we select HU values 25 and 45 as the thresholds. The corresponding steatosis degree distribution is shown in Fig. 2 (right). We also show the detailed statistical characteristics of each steatosis degree in Table 1.

4. Methodology

Our hepatic steatosis assessment model consists of two parts. First, we present the architecture of the body shape based network (Section 4.1). Second, we introduce the hybrid loss function to our model to increase the accuracy (Section 4.2).

4.1. Network architecture

Fig. 3 shows the architecture of the proposed S2FLNet with dilated

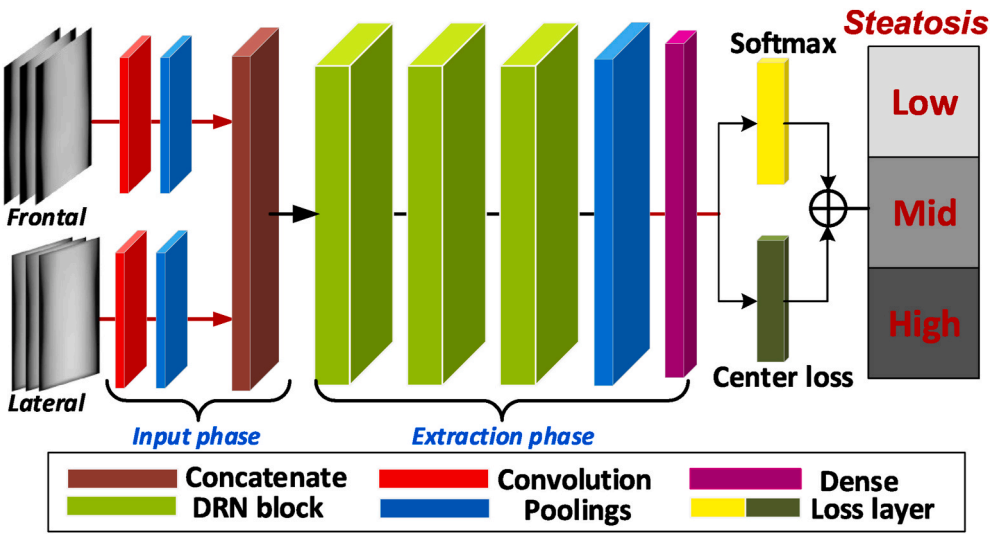

Fig. 3. The architecture of our proposed S2FLNet. The input phase of our network consists of two input channels: frontal and lateral body shape maps from Fig. 1. The strides of convolution and maxpooling layer in the input phase are set to 2. The extraction phase includes three DRN blocks with the same strides which is followed by a global average pooling layer and a fully connected layer.

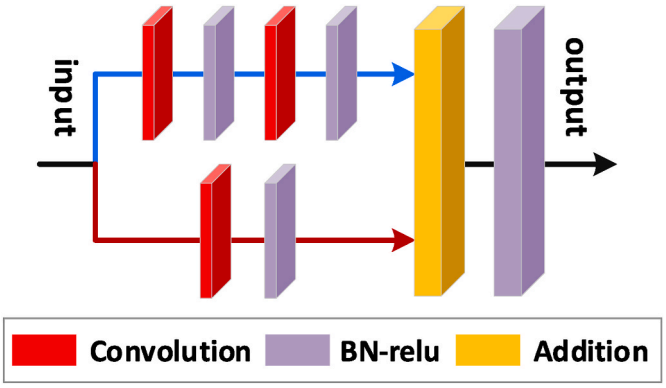

Fig. 4. The architecture of DRN block. The upper channel has two convolution layers and the lower channel has one convolution layer. All convolution layers adopt the dilated kernel with the same dilation rate and the strides of first convolution layer of the upper and lower channel are set to 2.0.

residual network (DRN) blocks [33,34] and center loss [35,36]. The proposed S2FLNet contains two inputs: frontal body shape map and lateral body shape map (From Fig. 1). The two input body shape maps are followed by two independent input phases with the same architecture. The first layer of the input phase consists of 3 × 3 dilated convolutional layers followed by a 3 × 3 max-pooling layer. Both layers of the input phase have a stride of 2.0, so their output size is 1/4 of the size of the input body shape maps. Then, the outputs of the two input phases are concatenated together through a concatenate layer. Next, three DRN blocks are introduced to extract deep and refined features. A global average pooling layer (GAP), a fully connected layer and a softmax are added successively after the last DRN block. DRN is taking advantage of the dilated convolution and the residual network. This kind of architecture is also proposed in Ref. [34] and increases the resolution of the ResNet blocks' output by replacing a subset of interior sub-sampling layers by dilation.

The receptive field of the network is one of the key factors that determines the representation power of feature maps in the convolutional layers [9,33]. Because the dimension of our input body shape maps is 512 × 512, our network needs a large receptive field to extract high resolution features. The general choices to expand the receptive field are enlarging the stripe of layers or increasing the depth of network. However, both of these approaches will introduce more trainable parameters and reduce the resolution so that more computational resources are needed. A neural network with more trainable parameters needs more data to avoid overfitting. However, it is difficult to get large medical data. The dilated convolution is just a convolution applied to input with defined gaps or holes between the kernel elements [33,37]. The dilated convolution is a way of acquiring a large receptive field without reducing the resolution or adding additional parameters. Therefore, the DRNs are able to represent both small and large image features and outperform the normal ResNet without adding algorithmic complexity to the model.

The three DRN blocks are exactly the same. Fig. 4 shows the architecture of our DRN blocks which consist of two channels that form the ResNet architecture. The convolution layers used in our DRN blocks adopt dilated kernel with the same dilation rate. In order to keep the output size consistent, the strides of the first convolution layer of the upper and lower channels are set to be the same value. In our work they are set to 2.0. Three DRN blocks are added following the input phase. The output size of the final DRN block is 1/32 of the input image size (e.g., in our model, the input dimension is 512 × 512. The output feature maps of the final DRN block is 16 × 16). For global contextual prior, average pooling is used before feeding to fully connected layers in image classification [34]. Therefore, we use GAP at the end of the DRN blocks and then feed the output feature maps to a fully connected layer.

The backbone of our network adopts structure of the form BatchNorm-ReLu [38]. The batch normalization following the convolution layer accelerates the training process by reducing internal covariate shift. The batch normalization also has the characteristic of regularization to reduce over-fitting which is especially suitable for the medical domain due to the limited data size. Overall, our network is well adopted to processing the high resolution inputs and the limited data which is prevalent in medical images.

4.2. Hybrid loss function

Cross entropy loss is one of the most popular loss functions employed in traditional deep classification networks [39]. However, cross entropy loss has a poor performance in generating discriminative features as it only encourages the separability of features [35,36]. Unlike general classification problems, the degrees of steatosis are very difficult to distinguish. In our study, we categorise the steatosis based on the HU values (proportional to the percentage of fat) of CT scan, as shown in

Fig. 2. Because HU value is continuous in the field, the bounds of the steatosis degrees are not absolutely separable. It is prone to mis-classify high (low) steatosis degree to low (high) steatosis degree, which is clinically unacceptable. Thus, we explore an effective loss function, center loss [36,40], which makes the classes close to their class center and compacts the intra-class variations. The details of the center loss function are as follows.

Suppose the training sample of the mini-batch is m and the number of classes is n. Let $f^1_{y_i}(x_i)$ be the output of pre-final layer before the fully connected layer by passing the ith training image (x_i) with label (y_i) through the network. Similarly, let $f^2_{y_i}(x_i)$ be the final fully connected layer output. Suppose class y_i has N_{y_i} images. First, the training images of the mini-batch are passed through the network. Next, we calculate the deep feature center (c_{y_i}) of the class y_i and the center loss $\mathcal{L}_{center}$ as formulated in Eq. (1):

$$\mathcal{L}_{center} = \sum_{i=1}^{m} \left\| f^1_{y_i}(x_i) - c_{y_i} \right\|_2^2, \quad \text{where } c_{y_i} = \frac{1}{N_{y_i}} \sum f^1_{y_i}(x_i). \tag{1}$$

The formulation effectively characterizes the intra-class variations.

When training the deep neural network, we apply the joint supervision of cross entropy loss $\mathcal{L}_s$ and center loss $\mathcal{L}_{center}$ to prevent the embedding from collapsing. The joint loss $\mathcal{L}_{total}$ is formulated in Eq. (2):

$$\begin{aligned} \mathcal{L}_{total} &= \mathcal{L}_s + \lambda \mathcal{L}_{center} \\ &= -\sum_{i=1}^{m} \log \frac{e^{W^T_{y_i} f^2_{y_i}(x_i) + b_{y_i}}}{\sum_{j=1}^{n} e^{W^T_j f^2_{y_i}(x_i) + b_j}} \\ &\quad + \lambda \sum_{i=1}^{m} \left\| f^1_{y_i}(x_i) - c_{y_i} \right\|_2^2, \end{aligned} \tag{2}$$

where W and b are the weight matrix and bias vector in the last fully connected layer respectively. W_j and W_{y_i} denote the jth and $y_i{}^{th}$ columns of W. b_j and b_{y_i} denote the jth and $y_i{}^{th}$ elements of b. Loss weight λ is a weight tuning parameter which balances the center loss and cross entropy loss. The optimal λ depends on the data and the task and requires tuning. One may select the optimal λ through analyzing different loss weights. More details can be found in Experiment. By minimizing the joint loss $\mathcal{L}_{total}$ with respect to W and b, we get the target softmax outputs.

5. Experiment

In this section, we carry out the proposed deep neural network on the dataset in Section 3.1 and evaluate the performance of hepatic steatosis classification.

5.1. Implementation

The proposed network with different parameters in this paper are implemented on the open source deep learning framework TensorFlow. To optimize the algorithm, the stochastic gradient descent optimizer with learning rate of 0.01 and momentum of 0.9 is used. We set the batch size to 16 to train the network and set the overall training phase to be 100 epochs. The training and validation processes are performed on two NVIDIA GTX 1080Ti graphics cards (11 GB GPU memory for each). TensorFlow offers a parameter called *class_weight* in model training that directly specifies the weight for each of the classes. To reduce the impact of the imbalance of the dataset, we set the parameter *class_weight* to equal the number of classes in the training process.

To evaluate the performance of each method comprehensively, we calculate the total classification accuracy, confusion matrix and area under curve (AUC) of the receiver operating characteristic (ROC) curve.

Due to the data size limitation of medical dataset, and to reduce the impact of particular random choice of samples, we use five-fold cross validation to evaluate the performance of the methods. In order to balance the testing and training data, we make training/testing ratios the same across of the degrees of steatosis.

Table 2
The results of ablation study.

Study	Parameters	Accuracy %
Dilation rate	1×1	76.3
	2×2	82.0
	3×3	78.7
	4×4	74.7
	5×5	74.3
Loss weight λ	0	72.3
	0.1	74.7
	0.2	82.7
	0.3	80.3
	0.4	77.3
	0.5	73.7

5.2. Ablation study

The dilation convolution rate and loss weight are the most important hyper-parameters in our network. In this section, we run ablation studies to isolate the effect of the dilated convolution and the center loss. We discuss various parameters and the methodology to find the optimal parameters of our network.

5.2.1. Dilated convolution

We discuss different dilation rates in our dilated convolution layers and observe how the dilated convolution influences the performance of our network. We run the network with different dilation rates (1×1, 2×2, 3×3, 4×4 and 5×5), where the dilation rate 1×1 means there is no dilated convolution and only classical convolutional layers are used. When discussing the dilation rates, we set the loss weight ($\lambda = 0.2$) in Eq. (2). The prediction accuracy with different dilation rates is shown in Table 2 (top). The ablation study results show that the dilated convolution in the network influences the classification accuracy. We observe that the performance can be improved if we select an appropriate dilation rate. The dilated convolution can expand the receptive field and extract more contextual information. Although a larger dilation rate can increase the receptive field, this may reduce the effectiveness of the filters and hurt the classification performance as well. Therefore, we select an optimal dilation rate to strengthen performance. Based on our study, the dilation rate 2×2 outperforms others (top blue row). Compared with the model without dilated convolution, our proposed network improves the accuracy by approximately 6% (from 76.3% to

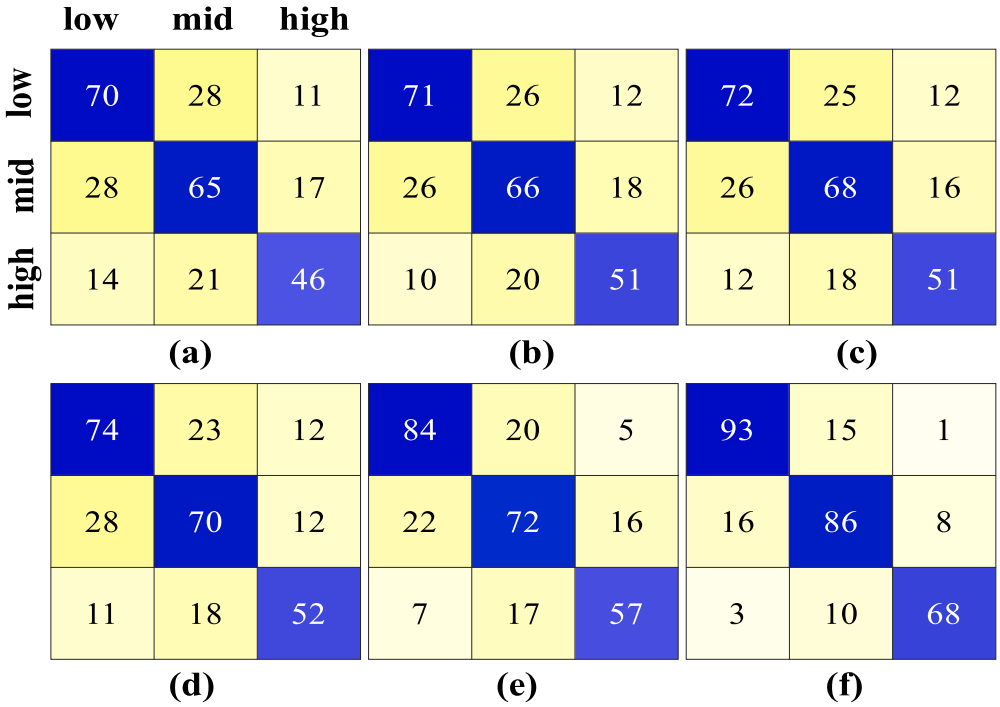

Fig. 5. The results of different classification methods. From (a)–(f): the confusion matrices are for Waist + Logistic Regression, Waist + SVM, 2D Body Shape + Logistic Regression, 2D body Shape + SVM, Baseline method and proposed S2FLNet.

82.0%).

5.2.2. Center loss

The other important characteristic of our proposed network is the hybrid center loss. Therefore, we want to know if and how the center loss

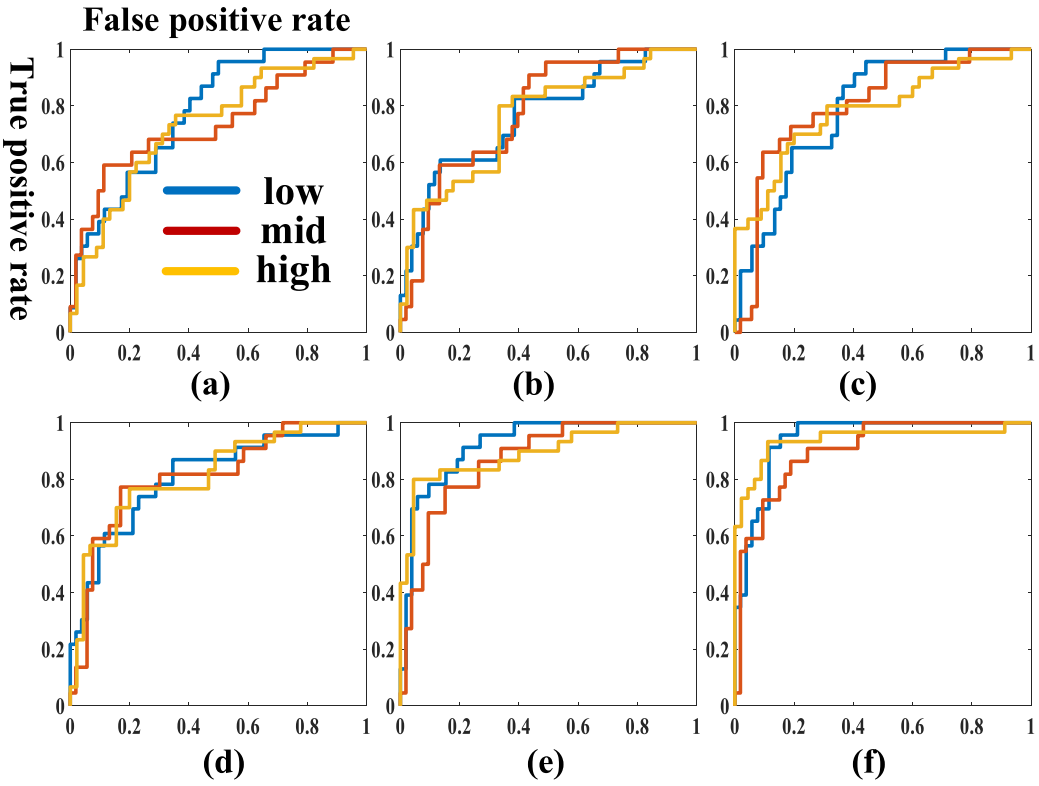

Fig. 6. The ROC curve results of different classification methods. From (a)–(f): the diagrams are for Waist + Logistic Regression, Waist + SVM, 2D body shapes + Logistic Regression, 2D body shapes + SVM, Baseline method and proposed S2FLNet.

Table 3
The classification performance comparison of different models on the public medical dataset.

Method	AUC			Accuracy %
	low	mid	high	
LR (Waist)	0.779	0.735	0.732	60.3
SVM (Waist)	0.767	0.780	0.759	62.7
LR (2D body shape)	0.794	0.806	0.787	63.7
SVM (2D body shape)	0.809	0.813	0.815	65.3
Baseline	0.922	0.868	0.895	71.0
S2FLNet	**0.951**	**0.905**	**0.940**	**82.3**

can improve the classification performance. We run the network with different loss weights $\lambda = (0, 0.1, 0.2, 0.3, 0, 4, 0.5)$, where the loss weight $\lambda = 0$ indicates that we do not embed center loss and only use traditional cross entropy loss. The dilation rate is fixed at 2×2. The results are shown in Table 2 (bottom). We can see that the introduction of center loss improves the accuracy significantly. It is worth noting that increasing loss weight does not always enhance the performance. The center loss can increase the intra-classes variation, but may make the classes cluster to the same center and decrease the inter-classes differences. In our study, the loss weights $\lambda = 0.2, 0.3$ work better than other loss weights and achieve a total accuracy of over 80% (bottom blue and gray rows refer to $\lambda = 0.2, 0.3$ respectively). Compared with the network without using center loss, the loss weight $\lambda = 0.2$ improves the accuracy by about 10% (from 72.3% to 82.7%).

The optimal parameters depend on the task and dataset. Based on our ablation study, we select the optimal dilation rate of 2×2 and loss weight $\lambda = 0.2$.

5.3. Comparison with reference methods

5.3.1. Performance experiment

To the best of our knowledge, this work is the first to explore the relationship between body shape and hepatic steatosis. Therefore, our major objective is to validate the proposed method which uses 2D body maps to predict hepatic steatosis. We have two specific aims: one is to verify the effectiveness of the body shape descriptors and the other is to validate the proposed network. There exists no other shape based methods to grade hepatic steatosis. The closest approach to ours is the use of waist circumference to predict steatosis [23]. Thus, we apply the LR and the linear SVM to model the relationship between waist circumference and hepatic steatosis. Furthermore, in order to evaluate the relative effectiveness of using 2D body shape maps, we also apply these two classical statistic methods (LR and SVM). The 2D body shape maps are not appropriate for direct use in SVM and logistic regression. Unlike convolutional neural network which has feature extraction and dimensionality reduction, the SVM and logistic regression cannot refine the high dimensional 2D body shape maps. Therefore, we apply PCA on our body shape maps and select the top principal components (PCs) of our body shape maps which characterize at least 95% of the variation in body shape. We also run the baseline method (the S2FLNet without using dilated convolution and center loss) in our experiment to validate the proposed neural network.

Fig. 5 and Fig. 6 show the confusion matrices and ROC curves of the different methods. The quantitative results of classical methods and networks are shown in Table 3. The LR and SVM using only waist circumference have the prediction accuracy of less than 63% (LR: 60.3%, SVM: 62.7%) which are worse than all body shape based approaches. The LR and SVM using our 2D body shape maps improve the total accuracy by about 3% (LR: 60.3% → 63.7%, SVM: 62.7% → 65.3%) compared with the same models using waist circumference. Both baseline and the proposed S2LFNet which adopt the deep neural network have significant advantages over the classical statistical models (blue row). This indicates that deep neural networks can extract more discriminative features than principal component analysis and classical statistical models. Furthermore, we can see that our proposed S2FLNet works the best in terms of both accuracy and AUC values. Compared with the baseline method, the proposed S2FLNet improves the total accuracy by about 11% (from 71.0% to 82.3%). According to the results of the confusion matrix, our proposed neural network outperforms the baseline without adding center loss and our misclassification between degrees low and high is very low. This has clinical significance. The center loss works well in our task because it compacts the intra-class variations.

The AUC values are used to evaluate the prediction performance of the classical statistical models and proposed neural networks. First, similar to the classification accuracy results, all AUC values of the waist related models are less than those of body shape based methods. Second, the AUC values of the baseline method and proposed S2FLNet are generally larger than those of LR and SVM in the three categories, which indicates that the deep neural networks have better predictability for hepatic steatosis. Third, the three AUC values of proposed S2FLNet are over 0.9 and are larger than those of the baseline method. This shows our S2LFNet archives the best predictability for hepatic steatosis with 2D body shape maps.

These experimental results demonstrate that the 2D body shape maps include more shape information and train better than waist circumference. Our proposed deep neural networks surpass the classical statistical models (LR, SVM) with the same body shape maps. In addition, according to the results of different network variations, the dilated convolution and the center loss can improve the prediction performance. Our proposed method promises to make diagnosing hepatic steatosis more affordable and convenient without compromising accuracy.

5.3.2. Visualization experiment

We conduct visualization experiments to investigate the discriminative body regions used by the deep neural network to identify hepatic steatosis. This is designed to give insight on the inner workings of the S2FLNet that would allow clinicians to interpret the “black box” often

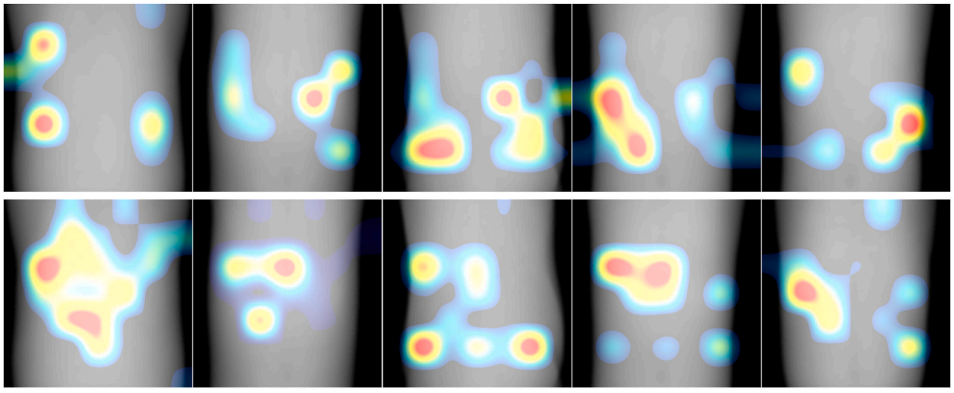

Fig. 7. Heatmap visualization. The Top row shows the heatmaps of the baseline approach and the bottom row shows the heatmaps of the proposed network overlaid on top of the frontal map of the body. The highlighted regions refer to the effective regions to predict steatosis degrees, the warmer color means higher correlation. (For interpretation of the references to color in this figure legend, the reader is referred to the Web version of this article.)

associated with machine learning approaches. Gradient-weighted Class Activation Mapping (Grad-CAM) [41] is a class-discriminative localization technique and could also be used to interpret the prediction decision made by the deep neural network. We generate the feature activation heatmap by Grad-CAM for both baseline network and the proposed network. The results are shown in Fig. 7. The baseline network exhibits a circumscribed activation on the sides of the abdomen which are not the best region for the prediction of hepatic steatosis [42,43]. The proposed S2FLNet generate a wide activation on the region where the liver is located. This indicates that our proposed network has the ability to learn from a rich representation of the body shape.

6. Conclusion

Unlike the current studies on hepatic steatosis assessment, we present a novel deep neural network based approach to determining the degree of hepatic steatosis using body shapes. Because of the high resolution of input body shapes and the difficulty of distinguishing the degrees of hepatic steatosis, our proposed network introduces the DRN blocks and the center loss to improve the classification performance. Classical methods and proposed network with various parameters (with/without dilated convolution and center loss) are tested on medical datasets. The optimal dilation rate and loss weight are chosen to achieve excellent accuracy. The experimental results show that our 2D body shape maps are better than simple waist circumference and the proposed deep neural networks are superior to classical methods, (e.g., SVM and LR). The network with dilated convolution and the center loss achieves the best prediction accuracy and AUC values. The detailed performance analysis indicates that our proposed S2FLNet solution provides a less-expensive and accurate alternative to competing solutions for assessing hepatic steatosis.

Our proposed method is limited in the following perspectives. First, our proposed method only utilized partial body shape information due to the fact that 2D body shapes are only available from two directions. Second, there are more shape representation approaches that can be used to extract shape information such as surface curvature and surface normal. Third, the approach presented here uses CT for both the body shape and the degree of steatosis. However, the approach can be used with shapes from any source including optical scans and steatosis degrees from liver biopsies.

Acknowledgements

This work was supported in part by the National Institutes of Health under grants R01DK129809 and the George Washington University Cross-Disciplinary Research Fund.

References

[1] P.J. Pickhardt, P.M. Graffy, S.B. Reeder, D. Hernando, K. Li, Quantification of liver fat content with unenhanced mdct: phantom and clinical correlation with mri proton density fat fraction, Am. J. Roentgenol. 211 (3) (2018) W151–W157.
[2] E. Goceri, Z.K. Shah, R. Layman, X. Jiang, M.N. Gurcan, Quantification of liver fat: a comprehensive review, Comput. Biol. Med. 71 (2016) 174.
[3] L. Abenavoli, L. Di Renzo, P.H. Guzzi, R. Pellicano, N. Milic, A. De Lorenzo, Non-alcoholic fatty liver disease severity, central fat mass and adinopectin: a close relationship, Clujul Med. 88 (4) (2015) 489.
[4] K. Clark, B. Vendt, K. Smith, J. Freymann, J. Kirby, P. Koppel, S. Moore, S. Phillips, D. Maffitt, M. Pringle, et al., The cancer imaging archive (tcia): maintaining and operating a public information repository, J. Digit. Imag. 26 (6) (2013) 1045–1057.
[5] F. Deeba, C. Schneider, S. Mohammed, M. Honarvar, E. Tam, S. Salcudean, R. Rohling, Swtv-ace: spatially weighted regularization based attenuation coefficient estimation method for hepatic steatosis detection, in: International Conference on Medical Image Computing and Computer-Assisted Intervention, Springer, 2019, pp. 610–618.
[6] T. Langner, R. Strand, H. Ahlström, J. Kullberg, Large-scale inference of liver fat with neural networks on UK biobank body mri, in: International Conference on Medical Image Computing and Computer-Assisted Intervention, Springer, 2020, pp. 602–611.
[7] P.R. Mendonça, P. Lamb, A. Kriston, K. Sasaki, M. Kudo, D.V. Sahani, Contrast-independent liver-fat quantification from spectral ct exams, in: International Conference on Medical Image Computing and Computer-Assisted Intervention, Springer, 2013, pp. 324–331.
[8] Z. Guo, G.M. Blake, K. Li, W. Liang, W. Zhang, Y. Zhang, L. Xu, L. Wang, J. K. Brown, X. Cheng, et al., Liver fat content measurement with quantitative ct validated against mri proton density fat fraction: a prospective study of 400 healthy volunteers, Radiology 294 (1) (2020) 89–97.
[9] Z. Yan, C. Tan, S. Zhang, Y. Zhou, B. Belaroussi, H.J. Yu, C. Miller, D.N. Metaxas, Automatic liver segmentation and hepatic fat fraction assessment in mri, in: International Conference on Pattern Recognition, IEEE, 2014, pp. 3280–3285.
[10] O.W. Hamer, D.A. Aguirre, G. Casola, J.E. Lavine, M. Woenckhaus, C.B. Sirlin, Fatty liver: imaging patterns and pitfalls, Radiographics 26 (6) (2006) 1637–1653.
[11] H. Dhami-Shah, R.A. Vaidya, et al., Non-alcoholic fatty liver disease: a practical guide, J. Obes. Metab. Res. 1 (1) (2014) 62.
[12] E.K. O'Neill, J.R. Cogley, F.H. Miller, The ins and outs of liver imaging, Clin. Liver Dis. 19 (1) (2015) 99–121.
[13] G. Bedogni, S. Bellentani, L. Miglioli, F. Masutti, M. Passalacqua, A. Castiglione, C. Tiribelli, The fatty liver index: a simple and accurate predictor of hepatic steatosis in the general population, BMC Gastroenterol. 6 (1) (2006) 1–7.
[14] L. Abenavoli, C. Luigiano, P. Guzzi, N. Milic, C. Morace, L. Stelitano, P. Consolo, S. Miraglia, S. Fagoonee, C. Virgilio, et al., Serum adipokine levels in overweight patients and their relationship with non-alcoholic fatty liver disease, Panminerva Med. 56 (2) (2014) 189–193.
[15] Y.N. Zhang, K.J. Fowler, G. Hamilton, J.Y. Cui, E.Z. Sy, M. Balanay, J.C. Hooker, N. Szeverenyi, C.B. Sirlin, Liver fat imaging—a clinical overview of ultrasound, ct, and mr imaging, Br. J. Radiol. 91 (1089) (2018) 20170959.
[16] Y. Lu, S. Zhao, N. Younes, J.K. Hahn, Accurate nonrigid 3d human body surface reconstruction using commodity depth sensors, Comput. Animat. Virtual Worlds 29 (5) (2018), e1807.
[17] Q. Wang, Y. Lu, X. Zhang, J.K. Hahn, A novel hybrid model for visceral adipose tissue prediction using shape descriptors, in: 2019 41st Annual International Conference of the IEEE Engineering in Medicine and Biology Society (EMBC), IEEE, 2019, pp. 1729–1732.
[18] X. Zhang, W. Xue, Q. Wang, Covariate balancing functional propensity score for functional treatments in cross-sectional observational studies, Comput. Stat. Data Anal. (2021) 107303.

[19] R. Ramírez-Vélez, M. Izquierdo, J.E. Correa-Bautista, M. Correa-Rodríguez, J. Schmidt-RioValle, E. González-Jiménez, K. González-Jiménez, Liver fat content and body fat distribution in youths with excess adiposity, J. Clin. Med. 7 (12) (2018) 528.
[20] A. De Lorenzo, V. Del Gobbo, M.G. Premrov, M. Bigioni, F. Galvano, L. Di Renzo, Normal-weight obese syndrome: early inflammation? Am. J. Clin. Nutr. 85 (1) (2007) 40–45.
[21] R.-N. Feng, S.-S. Du, C. Wang, Y.-C. Li, L.-Y. Liu, F.-C. Guo, C.-H. Sun, Lean-non-alcoholic fatty liver disease increases risk for metabolic disorders in a normal weight Chinese population, World J. Gastroenterol.: WJG 20 (47) (2014) 17932.
[22] S. Lee, F. Bacha, S.A. Arslanian, Waist circumference, blood pressure, and lipid components of the metabolic syndrome, J. Pediatr. 149 (6) (2006) 809–816.
[23] S. Lee, J.L. Kuk, C. Boesch, S. Arslanian, Waist circumference is associated with liver fat in black and white adolescents, Appl. Physiol. Nutr. Metabol. 42 (8) (2017) 829–833.
[24] Q. Wang, Y. Lu, X. Zhang, J. Hahn, Region of interest selection for functional features, Neurocomputing 422 (2020) 235–244.
[25] B.K. Ng, M.J. Sommer, M.C. Wong, I. Pagano, Y. Nie, B. Fan, S. Kennedy, B. Bourgeois, N. Kelly, Y.E. Liu, et al., Detailed 3-dimensional body shape features predict body composition, blood metabolites, and functional strength: the shape up! studies, Am. J. Clin. Nutr. 110 (6) (2019) 1316–1326.
[26] Q. Wang, W. Xue, X. Zhang, F. Jin, J. Hahn, Pixel-wise body composition prediction with a multi-task conditional generative adversarial network, J. Biomed. Inf. (2021) 103866.
[27] Y. Lu, J.K. Hahn, X. Zhang, 3d shape-based body composition inference model using a bayesian network, IEEE J. Biomed. Health Inform.. 24 (1) (2019) 205–213.
[28] H.R. Roth, L. Lu, A. Seff, K.M. Cherry, J. Hoffman, S. Wang, J. Liu, E. Turkbey, R. M. Summers, A new 2.5 d representation for lymph node detection using random sets of deep convolutional neural network observations, in: International Conference on Medical Image Computing and Computer-Assisted Intervention, Springer, 2014, pp. 520–527.
[29] X. Wang, S. Han, Y. Chen, D. Gao, N. Vasconcelos, Volumetric attention for 3d medical image segmentation and detection, in: International Conference on Medical Image Computing and Computer-Assisted Intervention, Springer, 2019, pp. 175–184.
[30] A.E. Kavur, M.A. Selver, O. Dicle, M. Barıs, N.S. Gezer, Chaos-combined (Ct-mr) Healthy Abdominal Organ Segmentation Challenge Data, 2019.
[31] P.A. Yushkevich, Y. Gao, G. Gerig, Itk-snap: an interactive tool for semi-automatic segmentation of multi-modality biomedical images, in: International Conference of the IEEE Engineering in Medicine and Biology Society (EMBC), IEEE, 2016, pp. 3342–3345.
[32] B. Ng, B. Hinton, B. Fan, A. Kanaya, J. Shepherd, Clinical anthropometrics and body composition from 3d whole-body surface scans, Eur. J. Clin. Nutr. 70 (11) (2016) 1265–1270.
[33] F. Yu, V. Koltun, Multi-scale Context Aggregation by Dilated Convolutions, arXiv Preprint arXiv:1511.07122.
[34] F. Yu, V. Koltun, T. Funkhouser, Dilated residual networks, in: Proceedings of the IEEE Conference on Computer Vision and Pattern Recognition, 2017, pp. 472–480.
[35] P. Ghosh, L.S. Davis, Understanding center loss based network for image retrieval with few training data, in: Proceedings of the European Conference on Computer Vision, ECCV), 2018, 0–0.
[36] Y. Wen, K. Zhang, Z. Li, Y. Qiao, A discriminative feature learning approach for deep face recognition, in: European Conference on Computer Vision, Springer, 2016, pp. 499–515.
[37] M. Anthimopoulos, S. Christodoulidis, L. Ebner, T. Geiser, A. Christe, S. Mougiakakou, Semantic segmentation of pathological lung tissue with dilated fully convolutional networks, IEEE J. Biomed. Health Inform. 23 (2) (2018) 714–722.
[38] S. Ioffe, C. Szegedy, Batch Normalization: Accelerating Deep Network Training by Reducing Internal Covariate Shift, arXiv Preprint arXiv:1502.03167.
[39] Z. Zhang, M. Sabuncu, Generalized cross entropy loss for training deep neural networks with noisy labels, in: Advances in Neural Information Processing Systems, 2018, pp. 8778–8788.
[40] C.-P. Tay, S. Roy, K.-H. Yap, Aanet: attribute attention network for person re-identifications, in: Proceedings of the IEEE Conference on Computer Vision and Pattern Recognition, 2019, pp. 7134–7143.
[41] R.R. Selvaraju, M. Cogswell, A. Das, R. Vedantam, D. Parikh, D. Batra, Grad-cam: visual explanations from deep networks via gradient-based localization, in: Proceedings of the IEEE International Conference on Computer Vision, 2017, pp. 618–626.
[42] J.T. Childs, A.J. Esterman, K.A. Thoirs, R.C. Turner, Ultrasound in the assessment of hepatomegaly: a simple technique to determine an enlarged liver using reliable and valid measurements, Sonography 3 (2) (2016) 47–52.
[43] F. Cervantes, J. Carbonell, M. Bruguera, L. Force, S. Webb, Liver disease in brucellosis. a clinical and pathological study of 40 cases, Postgrad. Med. 58 (680) (1982) 346–350.